



# Electrolytic deposition of super-smart composite coating of Zn-V<sub>2</sub>O<sub>5</sub>-NbO<sub>2</sub> on low carbon steel for defence application

O.S.I. Fayomi<sup>a, b</sup>, L.R. Kanyane<sup>a, \*</sup>, A.P.I. Popoola<sup>a</sup>, S.O. Oyedepo<sup>b</sup>

<sup>a</sup> Department of Chemical, Metallurgical and Materials Engineering, Tshwane University of Technology, P.M.B. X680, Pretoria, South Africa

<sup>b</sup> Department of Mechanical Engineering, Covenant University, P.M.B 1023, Ota, Nigeria

## ARTICLE INFO

### Article history:

Received 20 April 2018

Received in revised form

4 July 2018

Accepted 9 July 2018

Available online 10 July 2018

### Keywords:

Electrodeposition

Low carbon steel

Micro-hardness

Thermal stability corrosion behavior

Rare earth metal (REM)

## ABSTRACT

Despite the massive usages of low carbon steel in automobile for engineering components, its corrosion and high friction coefficient in aggressive environment make it limited in service. This paper is aimed at modifying low carbon steel structural component with thin film composite for enhanced mechanical and corrosion properties. The steel structure was electrodeposited with Zn-V<sub>2</sub>O<sub>5</sub> and embedded with varied NbO<sub>2</sub> weight concentration of 6–12 wt % based electrolyte. Scanning electron microscope (SEM) and high optical microscope was used to study the microstructural evolution of the fabricated coatings. The thermal stability of the fabricated coatings was studied in an isothermal furnace at 300 °C and 600 °C and further characterized using a high tech optical microscope. Potentiodynamic polarization technique was used to investigate the corrosion behavior of the composites in 3.65% NaCl. From the result, the effect of NbO<sub>2</sub> on Zn-V<sub>2</sub>O<sub>5</sub>-NbO<sub>2</sub> was massive with improved crystal grain within the coatings lattices. The coating possesses strong metallurgical bonding and good corrosion resistance properties of about 0.315 mm/yr corrosion rate compare to 4.1 mm/yr of as-received sample. No doubt the impact of thermal shock on the resilient characteristics of the composite coating was moderate owing to the stable adherent properties of the deposited coatings.

© 2018 Published by Elsevier Ltd. This is an open access article under the CC BY-NC-ND license (<http://creativecommons.org/licenses/by-nc-nd/4.0/>).

## 1. Introduction

The demand and applications of low carbon steel for different purposes especially in marine, construction and defence environment are mainly because of their excellent with resilient characteristic [1–3]. These properties such as malleability, ductility and welder-ability provide good mechanical properties even for extended application. However, the impact of corrosion and thermal shock on steel mostly affects the surface phenomenon which limits their applications in service leading to breakdown [4,5].

Zinc and zinc based are considered as effective methods employed for the corrosion protection of low carbon steel and resilient mitigation of surface against mechanical deformation [6–8]. In service, zinc deteriorates at steady chloride and acidified medium thereby devaluing its potential for stable protection [9–12]. The need for enhancement of existing zinc deposition

becomes necessary. Efforts on alternative materials have been carefully investigated by different researcher among which are Zn-SiO<sub>2</sub>, Zn-Al<sub>2</sub>O<sub>3</sub>, Zn-TiO<sub>2</sub>, Zn-Ni, Zn-Co alloy to mention but a few [13–16]. This composite embedded zinc coating had been found to provide good anti-corrosion properties when used as coating material on low carbon steel [17].

Niobium is a rare earth metal (REM), and are known to possess refractory characteristics. It is reported that Niobium forms a superficial oxide film and therefore its in-corporation into a composite coating for electrolytic deposition has been attested a potential improve corrosion [18]. Vanadium is used for high resistance dental implant. Vanadium oxides are capable of stabilizing a metal surface to prevent further oxidation when they form part of the coating [19–23].

Among many work done by different authors to improve the mechanical and corrosion properties of mild steel, there is no work open literature on Zn-V<sub>2</sub>O<sub>5</sub>-NbO<sub>2</sub> fabrication on mild steel via electrodeposition technique. Therefore, in this work, the micro-structure evolution, mechanical properties and corrosion resistance properties of Zn-V<sub>2</sub>O<sub>5</sub> become necessary in the presence of NbO<sub>2</sub> rare earth metal.

\* Corresponding author. Tel.: +27 12 382 4663.

E-mail addresses: [ojosundayfayomi3@gmail.com](mailto:ojosundayfayomi3@gmail.com) (O.S.I. Fayomi), [lrkanyane@gmail.com](mailto:lrkanyane@gmail.com) (L.R. Kanyane).

Peer review under responsibility of China Ordnance Society

**Table 1**  
Chemical composition of low carbon steel sample.

Element	C	Mn	Si	P	S	Al	Ni	Fe
wt %	0.18	0.45	0.18	0.01	0.031	0.005	0.008	99.19

## 2. Experimental procedures

### 2.1. Sample preparation and bath formulation

Mild steel sheets (40 mm × 40 mm × 2 mm) were selected as the substrate (cathode) for the experiment and the chemical composition of the mild steel is presented in Table 1. Substrate preparation involved mechanical polishing using grit SiC paper from a grit size of 40 μm–1200 μm. The anode was pure 99.99% commercial zinc with dimension of (60 mm × 60 mm × 5 mm).

The electrolytic bath and activating solution were prepared 24 h prior the experiment proper. The deposition was prepared with sulphate based constituent with activating solution of 0.5 M H<sub>2</sub>SO<sub>4</sub>. All deposition were done for 15 s with pH of 4 as described in Table 2. The chemicals used are Analar grade which were prepared using de-ionised water. The coating designed structure is presented in Table 3.

### 2.2. Morphological characterization

The structural evolution of the electrodeposited samples was characterized on Optical Microscope (OM) and Joel JSM6510 Scanning Electron microscopy (SEM).

### 2.3. Linear polarization resistance

The polarization resistance and corrosion rate measurements were taken using a μAutolab Type III Pontentiostat/Galvanostat. The polarization measurements were from a potential of –1.5 V to 1.5 V with scanning rate of 0.01 V/s. The circuit consisted of a saturated calomel electrode as a reference, graphite as a counter electrode and the coated samples as the working electrode.

### 2.4. Microhardness properties

The microhardness of the fabricated coatings layers were evaluated by means of micro vickers hardness tester under diamond based indentation loads of 100 gf. The indentation time was 10 s with four separate indentations taken at different measurement location within the surface interface.

## 3. Results and discussion

### 3.1. Morphological study

The surface micrographs of Zn-20V<sub>2</sub>O<sub>5</sub> and Zn-20V<sub>2</sub>O<sub>5</sub>-12NbO<sub>2</sub> matrix were characterized by SEM to obtain the structural

**Table 3**  
Deposition pattern of Zn-V<sub>2</sub>O<sub>5</sub>/NbO<sub>2</sub> alloy of fabricated samples.

Samples	Time	Current density	Potential/V
As received	—	—	—
Zn-20V <sub>2</sub> O <sub>5</sub>	15	2.5	1.0
Zn-20V <sub>2</sub> O <sub>5</sub> -6NbO <sub>2</sub>	15	2.5	1.0
Zn-20V <sub>2</sub> O <sub>5</sub> -12NbO <sub>2</sub>	15	2.5	1.0

evolution of the developed alloy. Fig. 1 clearly shows that the Zn-20V<sub>2</sub>O<sub>5</sub> coating surface evolution presented has small grains size with non-homogeneous and crystals at the interface. Although [11,12] attested that zinc coatings often possess inherent pores and cracks along the crystal buildup but this is invariably different from result obtained. The incorporation V<sub>2</sub>O<sub>5</sub> particles on Zn electrolyte improved the surface morphology of Zn based composite coatings. Moreover, Fig. 2 represent SEM image of Zn-V<sub>2</sub>O<sub>5</sub> with the addition of NbO<sub>2</sub> at different weight percent. Within the surface matrix of all embedded NbO<sub>2</sub> coating was an improved crystal evolution with compact grains noticed. The surface modification of the coatings can be credited to the incorporation of NbO<sub>2</sub> particulate which occupied up the gaps and the micro-holes of the coating lattice. Malatji et al. [11] stated that, the incorporation of nano particles in a coating stimulates increase in number of nucleation sites and crystal growth bringing about small-sized grains. According to [15], the impact of the rare earth metal (REM) inform of multigrain always result into a cohesive hexagonal crystal which is in par with a noticeable observation in this study as presented in Fig. 2(a) and (b). Although Fig. 2(b) gave a vivid coating with a superb uniform array of deposit compare to coating develop 6NbO<sub>2</sub> induced.

### 3.2. Microhardness examination

The hardness values of the substrate and zinc composite fabricated coatings are presented in Fig. 3. Improvement in microhardness can be noticed on all the composite coating samples compared to the control sample. An addition in NbO<sub>2</sub> nano-particle concentration in the bath solution on Zn-V<sub>2</sub>O<sub>5</sub> developed electrolyte resulted in enhancement of hardness potential. Although study by Ref. [13] mentioned that, metal matrix composite particles can lead to development of new microstructure and refinement in grain structure; hence causes maximum improvement in microhardness. This noticeable result is in par with the result obtained by Zn-V<sub>2</sub>O<sub>5</sub>-NbO<sub>2</sub> alloy developed. The presence of NbO<sub>2</sub> could be seen to contribute forcefully to the surface hard tendency of the substrate thereby resulting into appreciable hardness properties. No doubt Zn-V<sub>2</sub>O<sub>5</sub> displayed an appreciable coating performance in all regards but apparently not as ternary coating system with significant effect of about 190HVN. Surprisingly an increase in REM does not affect the microhardness performance of the coated samples positively, rather at 12 wt %, the microhardness properties of the fabricated samples decreased which is expected. Although [17] stated that multidoped coating often result into stable crystal refiner and not necessary on performance characteristics.

**Table 2**  
Bath Composition of Zn-V<sub>2</sub>O<sub>4</sub>-NbO<sub>2</sub> and operating condition.

Parameters	Composition	Mass concentration/(g·L <sup>-1</sup> )	pH	Voltage/V	Time/min	Temp./°C
Zn-V <sub>2</sub> O <sub>4</sub> -NbO <sub>2</sub>	ZnSO <sub>4</sub>	100	4	2	20.	40
	V <sub>2</sub> O <sub>5</sub>	20				
	NbO <sub>2</sub>	6/12				
	Boric acid	15				
	Sodium sulphate	20				
	Glycine	15				
	Thiourea	10				

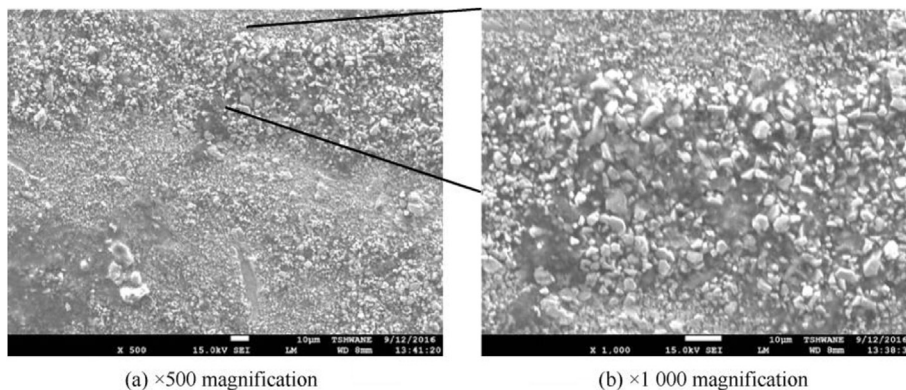


Fig. 1. SEM Micrographs of Zn-V<sub>2</sub>O<sub>5</sub> (a) × 500 magnification (b) × 1000 magnification.

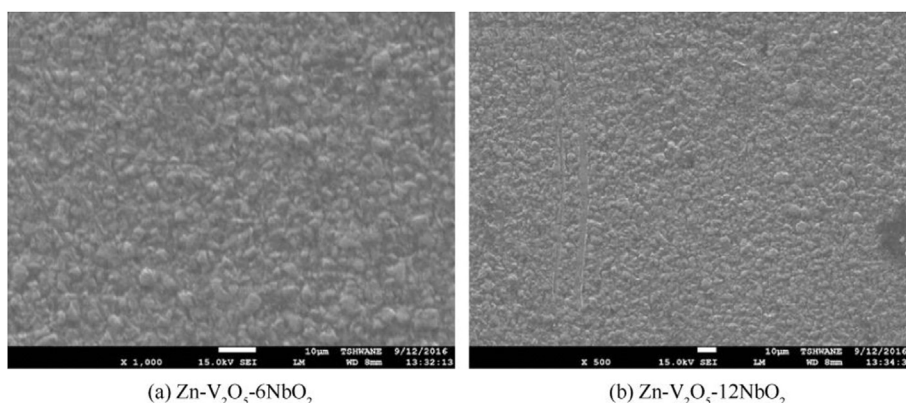


Fig. 2. SEM micrographs of (a) Zn-V<sub>2</sub>O<sub>5</sub>-6NbO<sub>2</sub> (b) Zn-V<sub>2</sub>O<sub>5</sub>-12NbO<sub>2</sub>.

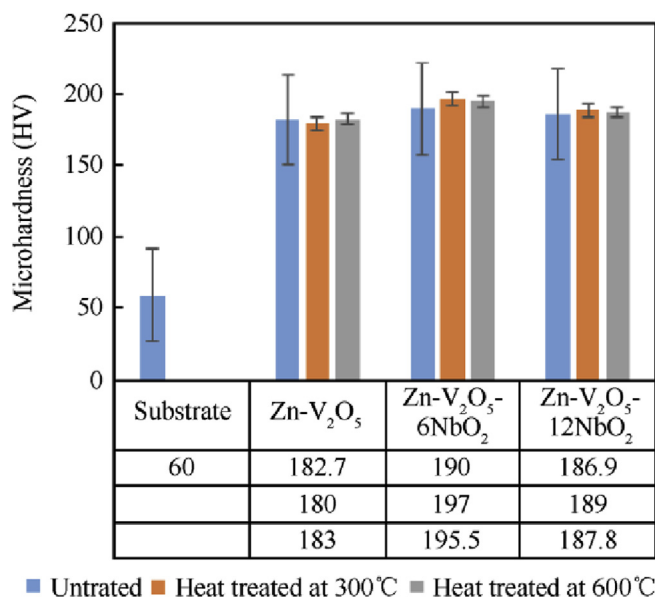


Fig. 3. Microhardness properties of Zn-V<sub>2</sub>O<sub>5</sub>/NbO<sub>5</sub> composite coatings.

More so in Fig. 3, examination of the thermal stability of the deposited coating were considered after an exposure to annealing process for 300 °C and 600 °C respectively for 3 h nanocomposite

via electrodeposits have been evaluated by following microhardness changes of the co-deposited samples as revealed by Fig. 4. The coatings were exposed to heat treatment at temperature of 300 °C and 600 °C respectively for 3 h. All coating maintain stability with high homogeneity which lead to slight increase in hardness tendency except for Zn-V<sub>2</sub>O<sub>5</sub> at 300 °C.

Figs. 4 and 5 shows the optical microstructures of samples after annealing at 300 °C and 600 °C respectively. It was seen that the microstructure appearance at 300 °C is finer and uniform with no evident of cracks at the interface. At 600 °C, stress initiation was noticed but not excessive. Although, an increased wt % of NbO<sub>2</sub> (12 wt %), Zn-V<sub>2</sub>O<sub>5</sub>-6NbO<sub>2</sub> there is no cracks observed at both temperatures. This is invariably indicated stable crystal growth and resilience to repeated thermal shock [18]. In general, there is a little increase in micro-hardness properties as compare to the samples without heat-treatment.

### 3.3. Linear polarization resistance

Figs. 6 and 7 display the polarization resistance (Ω) and corrosion rate (mm/year) respectively. The performance of the fabricated coatings on mild steel in the 3.65% NaCl solution was examined. The results achieved from Fig. 3 indicate that an increase in addition of NbO<sub>2</sub> elevates the polarization resistance of the Zn-20V<sub>2</sub>O<sub>5</sub> composite samples toward more positive region. Low carbon steel samples (uncoated sample) possess lowest polarization resistance of 27.6 Ω. Moreover, the highest polarization (R<sub>p</sub>) of 215.9 Ω is attained at for Zn-V<sub>2</sub>O<sub>5</sub>-12NbO<sub>2</sub>, followed by Zn-20V<sub>2</sub>O<sub>5</sub>-6NbO<sub>2</sub>

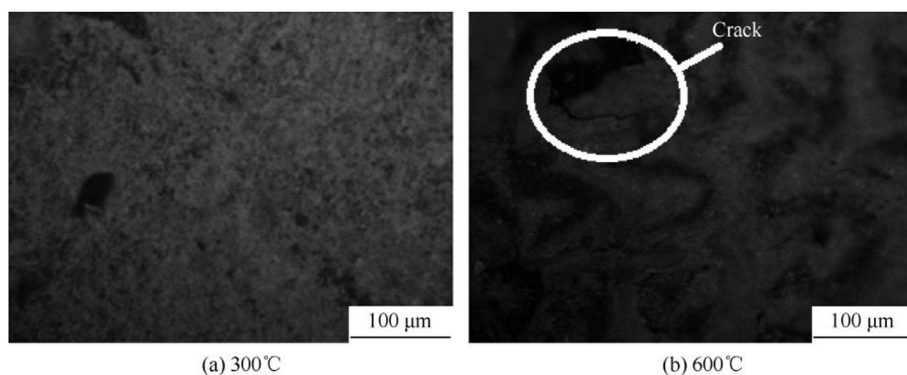


Fig. 4. Micrographs of the heat treated composite coatings on mild steel Zn-20V<sub>2</sub>O<sub>5</sub>-6NbO<sub>2</sub>.

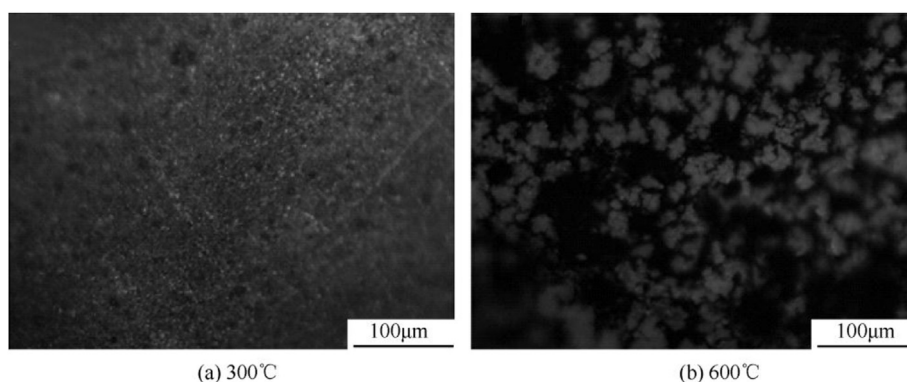


Fig. 5. Micrographs of the heat treated composite coatings on mild steel Zn-20V<sub>2</sub>O<sub>5</sub>-12NbO<sub>2</sub>.

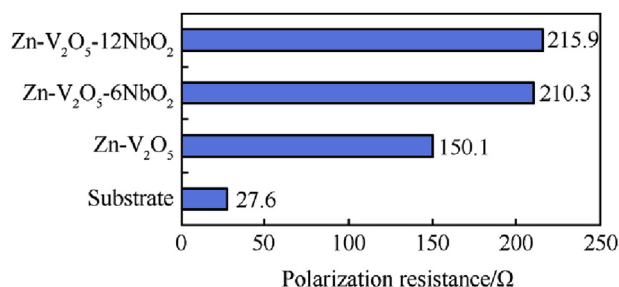


Fig. 6. Polarization resistance progression of coated alloys in 3.65% NaCl concentration at room temperature.

and Zn-20V<sub>2</sub>O<sub>5</sub> respectively. Material corrosion can be correlated to important factors such as chemical composition of the phase formed and grain size of the microstructural evolution. It is obvious that the maximum polarization resistance associated with 12 wt % NbO<sub>2</sub> is due to the fact that NbO<sub>2</sub> is more resistance to corrosion [20]. As expected, the substrate sample (uncoated mild steel) shows highest corrosion rate of 4.1 mm/year as compared to all fabricated samples. The addition of NbO<sub>2</sub> at varying content shows a greater impact on the corrosion rate of the matrix. At a point where NbO<sub>2</sub> is 12 wt %, the corrosion rate of the sample was lowest (0.315 mm/year).

The micrographs of the deposits after corrosion are shown in Fig. 8. The most distinct difference between the initial coatings is the pitting effect. The presence of pits across in Zn-V<sub>2</sub>O<sub>5</sub> shows that there is a tendency of erosion propagation over time. Fig. 8(b) also

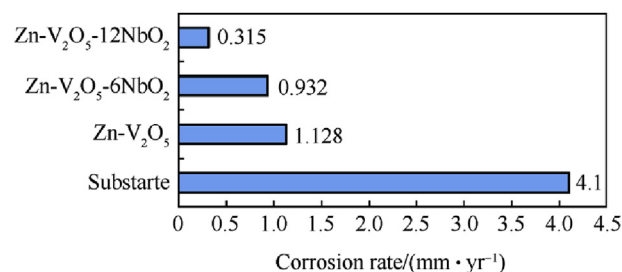


Fig. 7. Corrosion rate evolution of coated alloys in 3.65% NaCl concentration at 25 °C.

shows no significant corrosion product at the interface as expected with Zn-20V<sub>2</sub>O<sub>5</sub>-12NbO<sub>2</sub>. The better resilient corrosion propagation of Zn-20V<sub>2</sub>O<sub>5</sub>-12NbO<sub>2</sub> coating presented is attributed to good adhesion and compact grains for the deposited coatings [24].

#### 4. Conclusions

- (1) Zn-V<sub>2</sub>O<sub>5</sub>/NbO<sub>2</sub> was successfully electrodeposited on low carbon steel.
- (2) NbO<sub>2</sub> proved to be good grain refiner and potential for usage for extended application
- (3) Fabricated composite coating matrix of Zn-V<sub>2</sub>O<sub>5</sub>-12NbO<sub>2</sub> revealed improved corrosion resistance as compared to the substrate
- (4) Electrodeposited composite coatings resulted in increased microhardness properties of over 190 HVN.



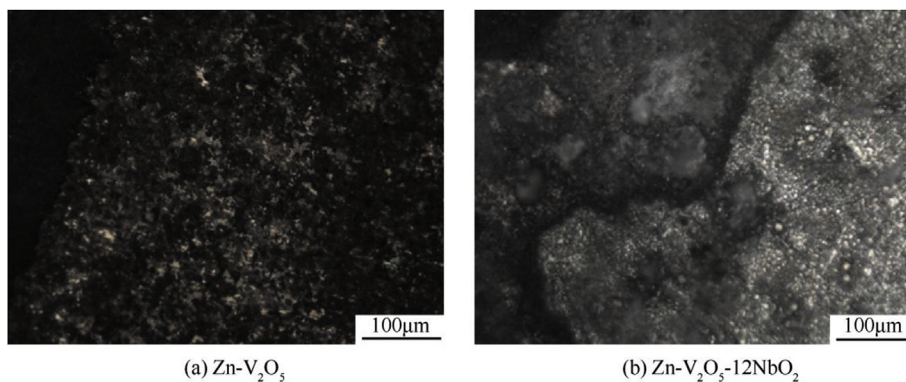


**Fig. 8.** (a) Zn-V<sub>2</sub>O<sub>5</sub> (b) Zn-V<sub>2</sub>O<sub>5</sub>-12NbO<sub>2</sub> micrographs after corrosion in 3.65%NaCl.

### Acknowledgements

The authors gratefully acknowledge Surface Engineering Research Centre (SERC), the Tshwane University of Technology, Department of Chemical Metallurgical and Materials Engineering, Pretoria, South Africa.

### References

- [1] Callister WD. Materials science and engineering: an introduction. seventh ed. New York: John Wiley & Sons; 2007.
- [2] Fayomi OSI, Popoola API, Aigbodion VG. J Alloy Comp 2015;623:328–34.
- [3] Fayomi OSI, Popoola API, Aigbodion VG. J Alloy Comp 2014;617:561–6.
- [4] Fayomi OSI, Popoola API. J Alloy Comp 2015;637:382–92.
- [5] Fratari RQ, Robin A. ElectrochimicaActa 2016;129:312–7.
- [6] Li Q, Lu H, Cui J, An M, Li D. Surf Coating Technol 2016;304:567–73.
- [7] Mamun MA, Zhang K, Baumgart H, Elmustafa AA. Appl Surf Sci 2015;359:30–5.
- [8] Malatji N, Popoola API, Fayomi OSI, Loto CA. Int J Adv Manuf Technol 2016;82:1335–41.
- [9] Popoola API, Aigbodion VG, Fayomi OSI. Surf Coating Technol 2016;306:448–54.
- [10] Popov BN. Corrosion engineering. first ed. Amsterdam: Elsevier; 2015.
- [11] Monyai T, Fayomi OSI, Popoola API. Procedia Manufacturing 2017;7:537–41.
- [12] Monyai T, Fayomi OSI, Popoola API. Data in brief, 2018, vol. 17; 2018. p. 757–62.
- [13] Monyai T, Fayomia OSI, Popoola API. A novel effect of Solanum Tuberosum/ Zn-30Al-7Ti sulphate modified coating on UNS G10150 mild steel via dual-anode electrodeposition route. Port Electrochim Acta 2016;34(5):35.
- [14] Fayomi OSI, Popoola API, Kanyane LR, Monyai T. Development of reinforced in-situ anti-corrosion and wear Zn-TiO<sub>2</sub>/ZnTiB<sub>2</sub> coatings on mild steel Results in physics, 2017, vol. 7; 2017. p. 644–50.
- [15] Costa MV, Oliveira CT, Dalla Corte DA, Rieder S, Muller IL, de FragaMalfatti C. Coatings for Corrosion Protection 2010;29:113.
- [16] Anawe PAL, Fayomi OSI. Results in Physics 2017;7:777–88.
- [17] Hosford WF. Materials for engineers. first ed. New York: Cambridge University Press; 2008.
- [18] Anawe PAL, Fayomi OSI. Port Electrochim Acta 2017;35(5):297–303.
- [19] Anawe PAL, Fayomi OSI, Ayodeji AA, Popoola API. Results in Physics 2018;9:1570–1. June 2018.
- [20] Anawe PAL, Fayomi OSI. Impact of metal matrix composite on the evolution and erosion performance characteristics of non lubricated-dry abrasive degradation of ternary composite. Results in Physics 2018;9:1215–23. June 2018.
- [21] Low CTJ, Wills RGA, Walsh FC. Surf Coating Technol 2006;201:371–83.
- [22] Anawe PAL, Raji O, Fayomi OSI. Influence of composite nano coating on ternary sulphate Co-deposition: corrosion and surface characterization. Procedia Manufacturing 2017;7:556–61. 2017.
- [23] Fayomi OSI, Popoola API, Oloruntoba T, Ayoola AA. Cogent Engineering 2017;4. 1318736 <https://doi.org/10.1080/23311916.2017.1318736>.
- [24] Fayomi1 OSI, Popoola1 API, Ige T, Ayoola AA. Asian J Chem 2017;29(12): 2575–81.